Int J Adv Manuf Technol (2016) 85:2037–2047
DOI 10.1007/s00170-015-7933-1

ORIGINAL ARTICLE

Effect of non-electrical parameters in μED milling: an experimental investigation

J. M. Jafferson[1] · **P. Hariharan**[2] · **J. Ram Kumar**[3]

Received: 22 February 2015 / Accepted: 2 October 2015 / Published online: 12 October 2015

Abstract Machining of high aspect ratio micro-channels and cavities in metals is a challenging task. Micro-electrical discharge milling is a version of micro-electrical discharge machining process which is capable of micro-machining of all electrically conductive materials. The aim of this study is to analyze the effects of non-electrical parameters such as layer thickness (LT), horizontal tool feed rate (HTF), and tool rotational speed (TRS) on material removal rate (MRR) and relative electrode wear (REW) while micro-electrical discharge (μED) milling of stainless steel using tungsten electrode. The study revealed that layer thickness along with tool rotational speed and horizontal feed rate of the tool significantly influences the performance of μED milling.

Keywords Micro-channel · Micro-EDM · Layer thickness · MRR · TWR · REW

1 Introduction

Micro-cavities and micro-channels are widely used in micro-reactors, biomedical micro-fluidics, etc. Machining of burr-free micro-channels with conventional micro-milling cutters is difficult. Although micro-electrical discharge machining (EDM) milling is a slow process, it is capable of producing burr-free micro-channels with very high precision and quality, which attracted researchers to focus on this area of micro-machining. The machining process parameters in μEDM decide the efficiency, precision, and quality of the micro-channels produced. The electrical machining parameters in μED milling are voltage, capacitance, and discharge energy. Discharge energy can be varied by altering the values of voltage and capacitance. The non-electrical machining parameters are layer thickness (LT) and tool rotational speed (TRS). Table 1 shows the input and output parameters analyzed by various researchers while μED milling. Minh et al. [1] analyzed the three different possible modes (micro-EDM/simultaneous electrical discharge chemical machining/micro-electrochemical milling) of machining while using deionized water as dielectric. The authors successfully explained the theory and shown the parameter settings required for all three modes of machining while following a layer-by-layer (0.2, 0.5, and 1 μm) based machining approach. The authors also varied horizontal feed rate of the tool and helped to visualize the parameter settings in which transition of micro-electrochemical machining (ECM) and micro-EDM happens.

Karthikeyan et al. [4] analyzed the process parameters like tool rotational speed, feed rate, and aspect ratio while machining EN 24 using tungsten tool. The authors reported the positive effects of tool rotation in helping the effective removal of debris. The authors also noticed that the material removal rate (MRR) is lower for even higher discharge energies while machining with low tool rotational speeds and also noticed the formation of very large-sized debris particles while machining with low

✉ J. M. Jafferson
jaffceg@gmail.com

P. Hariharan
hari@annauniv.edu

J. Ram Kumar
jramkuar@iitk.ac.in

[1] School of Mechanical and Building Sciences, Vellore University-Chennai campus, Chennai 600127, India

[2] Department of Manufacturing Engineering, CEG, Chennai 600025, India

[3] Mechanical Engineering Department IIT, Kanpur 208016, India

Table 1 μED milling performance based on electrical/non-electrical process parameters

Input parameters	Output parameters	References
Horizontal feed rate, layer thickness	Transition from μEDM to μECM	[1]
Layer depth, scanning feed rate	Machining accuracy	[2]
Discharge energy, layer thickness	Material removed per discharge	[3]
Feed rate, RPM, aspect ratio	Efficiency	[4]
RPM, discharge energy	Surface analysis (Ra)	[5]
RPM, feed rate, aspect ratio, discharge energy	Recast layer, surface analysis	[6]
Voltage, capacitance, discharge energy	TWR, Ra	[7]
Voltage, capacitance, feed rate	MRR, TWR, Ra, Ry	[8]

speed and feeds. The authors conducted detailed microscopic investigation on tool and workpiece surfaces for different parameter settings. Karthikeyan et al. [6] also conducted a detailed microscopic study on the effect of tool rotation while μED milling of EN 24 using tungsten tool. The authors reported that the tool rotation reduces the amount of tool material deposited on the surface of the workpiece.

1.1 Principle of μEDM

The basic material removal mechanism in μEDM resembles EDM. When a potential difference is applied (pulse-on time) between the tool (negative terminal) and workpiece (positive terminal) separated by a gap which are immersed in a dielectric medium, an electric field will be established in the gap and the electrons emitted from negatively charged electrode collide with neutral atoms in the inter-electrode gap and splits them into positive and negatively charged particles [9], which results in formation of more and more electrons and ions (ionization). The negatively charged particles will be attracted to the positive electrode and vice versa. The weight of a positive ion is more than thousand times heavier compared to the weight of an electron, so it accelerates much slower than the electrons. Since only a small number of positive ions hit the tool surface and a larger number of electrons bombard the workpiece surface during sparking, more materials are removed from the workpiece [10]. The electrons will be accelerated and collide with the neutral atoms in the dielectric fluid, and thus, more positive ions and electrons will get generated. This cyclic process increases the concentration of electrons and ions in the dielectric medium between the inter-electrode gap [11] to form plasma which has very low electrical resistance, and a large number of electrons will flow from the tool to workpiece and ions from the workpiece to the tool causing avalanche motion of electrons which can be seen as a spark [12]. The kinetic energy of the electrons and ions on impact with the surface of the workpiece and tool, respectively, would be converted into thermal energy or heat flux. Such intense localized heat flux [13] leads to extreme instantaneous confined rise in temperature which would be in the range of 8000 to 10,000 K [14], which melts and vaporizes the material instantly. When the potential difference is withdrawn (pulse-off time), the plasma channel collapses generating pressure or shock waves [15], which evacuates the molten material forming a crater of removed material around the site of the spark. Also, deionization occurs during the pulse-off time so that there will be no overheating of the workpiece due to continuous arcs [16]. When the debris particles are accumulated in the bottom and the sides of the tool, a conductive bridge will be developed which results in increase of heat generation and short circuiting; the tool feed rate will get adjusted automatically to overcome short circuiting which results in very fast retractions resulting in an oscillatory motion of the tool [17], which is expected to produce pumping action which helps to remove the debris from the inter-electrode gap [18]. The literatures explain that the material removal mechanism in μEDM is dominated by melting action in higher discharge energies, but at lower discharge energies, the material is removed by vaporization [19, 20]. The desirable properties of μEDM tool material are very high electrical conductivity, high melting point, high thermal conductivity, and higher density. The most commonly used electrode materials in μEDM are brass, copper, tungsten, copper tungsten, and silver tungsten. Micro-EDM resembles macro-EDM in working principle, but it differs much in other parameters. In EDM, the erosion rate is maximized [21] by selecting optimal pulse parameters and current characteristics but the objective of μEDM is to minimize the quantity of material eroded in the workpiece per single discharge.

2 Research GAP

Corner tool wear and tool taper are the common problems in μED milling which severely affects the precision. A layer-by-layer machining approach overcomes this problem so that the tool tip dressing is not needed

and there is negligible tool taper. Works reported on layer-by-layer machining approach in μED milling are very few.

Bissacco et al. [3] demonstrated the reliability of a method to compensate the tool wear by analyzing the material removed per discharge with the help of

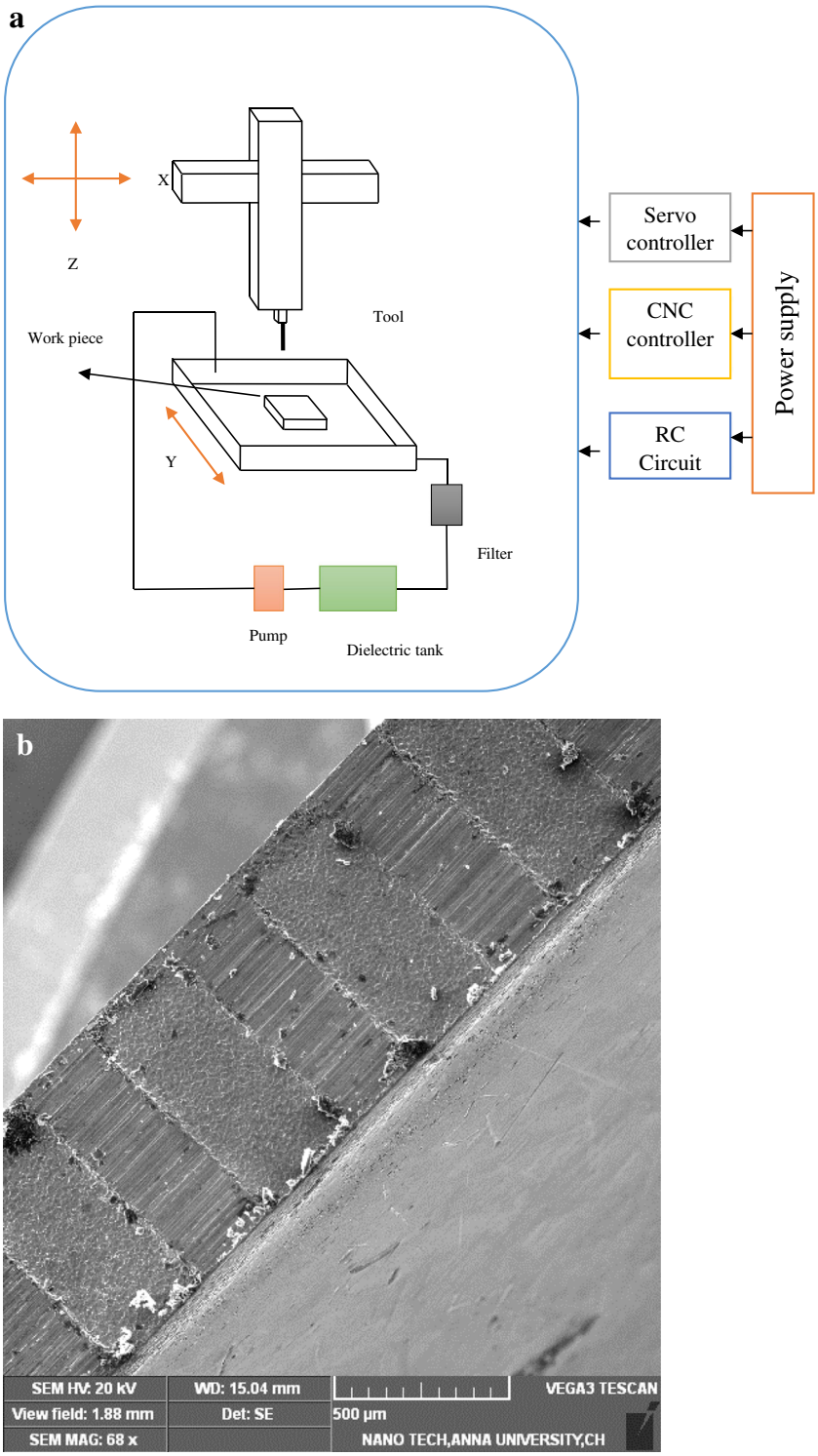

Fig. 1 **a** Arrangement of various components of the μEDM setup. **b** SEM image of the rectangular slots machined

Table 2 Properties of workpiece/tool materials

Properties	AISI 304	Tungsten
Melting point (°C)	1450	3370
Electrical resistivity (nΩ m)	720	52.8
Thermal conductivity (W/m K)	16.2	173
Density (g/cm^3 at 25 °C)	8	19.3
Coefficient of thermal expansion ($\alpha(10^{-6}$ K^{-1}))	17.3	4.5
Specific heat capacity (J/kg K)	500	170

counting the discharges and comparing with the online measurement of material removed per discharge while machining martensitic stainless steel with tungsten carbide tool with a layer-by-layer machining approach (0.5, 0.9, and 2.5 μm). They found that this method is very efficient while machining with low discharge energy parameter settings. Dang et al. [22] analyzed the three different possible modes (micro-EDM/SEDCM/micro-ECM milling) of machining while using deionized water as dielectric. They successfully demonstrated the theory and parameter settings required for all three modes of machining while following a layer-by-layer (0.2, 0.5, and 1 μm) based machining approach. The authors also varied horizontal feed rate of the tool and helped to visualize the parameter settings in which micro-ECM and micro-EDM happen.

From the literature survey, it was observed that there are no publications reporting the combined effects of the non-electrical parameters like layer thickness, tool rotational speed, and horizontal tool feed rate with respect to MRR and relative electrode wear (REW) in μED milling. REW is the ratio of the volume of material removed from the tool electrode to the volume of material removed from the workpiece. If the value of REW is lower, then it means that the life of tool is higher. This study analyzes the impact of LT, horizontal tool feed rate (HTF), and TRS in MRR and REW.

3 Experimental setup

A multi-purpose micro-machining tool DT110 equipped with RC-type pulse generator was used for conducting the μEDM milling experiments. The line diagram of the experimental setup is shown in Fig. 1a.

The stainless steel (AISI 304) was used as workpiece material and cylindrical tungsten rod (0.3-mm dia) as tool electrode. AISI 304 is a corrosion-resistant, non-magnetic, and difficult to machine material and has

Table 3 Tabulated values of TWR, MRR and relative electrode wear when layer thickness (LT), tool rotational speed (*S*), and horizontal tool feed rate (HTF) are varied

Sl. no.	*S* (rpm)	HTF (mm/min)	LT (μm)	MRR μm^3/min	TWR μm^3/min	Relative electrode wear
1	100	10	0.5	1534	657	0.40
2	750	10	0.5	2166	506	0.20
3	1500	10	0.5	3001	574	0.19
4	2500	10	0.5	3896	506	0.12
5	100	40	0.5	8201	1566	0.19
6	750	40	0.5	16,019	2852	0.17
7	1500	40	0.5	25,201	3867	0.15
8	2500	40	0.5	16,513	2417	0.14
9	100	70	0.5	12,759	2028	0.15
10	750	70	0.5	25,059	4600	0.18
11	1500	70	0.5	31,790	4153	0.13
12	2500	70	0.5	35,474	4561	0.12
13	100	100	0.5	12,927	740	0.05
14	750	100	0.5	38,649	2081	0.05
15	1500	100	0.5	46,477	3032	0.06
16	2500	100	0.5	58,355	2724	0.04
17	100	10	1	3614	1050	0.29
18	750	10	1	4761	1353	0.28
19	1500	10	1	5785	1334	0.23
20	2500	10	1	4484	1663	0.37
21	100	40	1	5995	4813	0.80
22	750	40	1	28,318	4410	0.15
23	1500	40	1	32,319	4195	0.12
24	2500	40	1	34,653	5353	0.15
25	100	70	1	24,451	2704	0.11
26	750	70	1	37,909	4543	0.11
27	1500	70	1	44,432	4965	0.11
28	2500	70	1	44,047	4808	0.10
29	100	100	1	24,395	1405	0.05
30	750	100	1	53,866	3438	0.06
31	1500	100	1	54,381	3009	0.05
32	2500	100	1	63,314	3447	0.05
33	100	10	1.5	1500	640	0.42
34	750	10	1.5	2116	500	0.23
35	1500	10	1.5	2854	560	0.19
36	2500	10	1.5	3876	480	0.12
37	100	40	1.5	8136	1432	0.17
38	750	40	1.5	15,526	2578	0.16
39	1500	40	1.5	25,006	2624	0.10
40	2500	40	1.5	16,361	2265	0.13
41	100	70	1.5	12,432	2001	0.16
42	750	70	1.5	24,797	4576	0.18
43	1500	70	1.5	31,522	4089	0.12

Table 3 (continued)

Sl. no.	*S* (rpm)	HTF (mm/min)	LT (μm)	MRR μm³/min	TWR μm³/min	Relative electrode wear
44	2500	70	1.5	35,022	4457	0.12
45	100	100	1.5	12,562	724	0.05
46	750	100	1.5	38,135	2002	0.05
47	1500	100	1.5	45,006	2986	0.06
48	2500	100	1.5	55,014	2547	0.04
49	100	10	2	1439	630	0.44
50	750	10	2	2005	480	0.24
51	1500	10	2	2632	530	0.20
52	2500	10	2	3765	444	0.12
53	100	40	2	7895	1407	0.18
54	750	40	2	11,590	2375	0.20
55	1500	40	2	14,624	2436	0.17
56	2500	40	2	16,060	2107	0.13
57	100	70	2	17,506	1944	0.11
58	750	70	2	23,335	4168	0.18
59	1500	70	2	29,655	3879	0.13
60	2500	70	2	24,543	4134	0.17
61	100	100	2	12,035	708	0.06
62	750	100	2	37,657	1876	0.05
63	1500	100	2	44,565	2568	0.06
64	2500	100	2	53,569	2298	0.04

numerous applications. Tungsten is suitable for μED milling because of its very low tool wear rate compared to brass and copper. The properties of the tool and workpiece materials used are given in Table 2. Voltage and capacitance values were fixed at 100 V and 10 nF based on experience, and a full factorial experiment was conducted by considering four different levels of LT (0.5, 1, 1.5, and 2 μm), TRS (100, 750, 1500, and 2500 rpm), and HTF (10, 40, 70, and 100 mm/min) and were varied based on hardware limitations. Thus, a total of 64 (4×4×4=64) experimental runs were conducted, considering the full factorial at four different levels of each factor, and the results are tabulated in Table 3. The reason for conducting such a large number of experiments using full factorial design is to analyze if there is any interaction between the factors. The length, width, and depth of the micro-channel are dimensions of the machined rectangular micro-channels that are 1000, ≈800, and 50 μm. A sample SEM image of the micro-channels machined is shown in Fig. 1b.

4 Results and discussion

The experimental runs were conducted randomly, and statistical analysis of variance was conducted for both MRR and REW (Tables 4 and 5) using Minitab 17 software, and the corresponding main effect plot and interaction plots are shown in Figs. 2, 3, 4, and 5. Since the calculated value of F is larger than the standard value of F and also the P values are less than 1, the null hypothesis (LT, HFT, TRS, and their interaction does not affect MRR) is rejected and concluded that LT, HFT, TRS, and their interactions excluding the interaction of TRS versus LT significantly affects MRR. REW is influenced by HTF and LT because only for these two parameters, the calculated value of F is larger than the standard value of F.

Table 4 Analysis of variance MRR

Source	DF	SS	MS	F_{calc}	$F_{0.05;(v1, v2)}$	P	Contribution
Model	36	20157559087	559932197	33.05	1.852457468	0.000	97.78 %
Linear	9	17502818465	1944757607	114.80	2.250131477	0.000	84.90 %
TRS (rpm)	3	3523389272	1174463091	69.33	2.960351318	0.000	17.09 %
HTF (mm/min)	3	12470388354	4156796118	245.37	2.960351318	0.000	60.49 %
LT (μm)	3	1509040840	503013613	29.69	2.960351318	0.000	7.32 %
Two-way interactions	27	2654740622	98323727	5.80	1.904822988	0.000	12.88 %
TRS (rpm) × HTF (mm/min)	9	2037098399	226344267	13.36	2.250131477	0.000	9.88 %
TRS (rpm) × LT (μm)	9	77867384	8651932	0.51	2.250131477	0.854	0.38 %
(mm/min) × LT (μm)	9	539774839	59974982	3.54	2.250131477	0.005	2.62 %
Error	27	457406285	16940974				2.22 %
Total	63	20614965372					100.00 %

Table 5 Analysis of variance REW

Source	DF	SS	MS	F_{calc}	$F_{0.05;(v1, v2)}$	P	Contribution
Model	36	4.189	0.116367	1.23	1.852457468	0.289	62.18 %
Linear	9	2.27	0.252659	2.68	2.250131477	0.023	33.75 %
TRS (rpm)	3	0.19423	0.064744	0.69	2.960351318	0.568	2.88 %
HTF (mm/min)	3	1.01777	0.339257	3.59	2.960351318	0.026	15.11 %
LT (μm)	3	1.06193	0.353977	3.75	2.960351318	0.023	15.76 %
Two-way interactions	27	1.91527	0.070936	0.75	1.904822988	0.768	28.43 %
TRS (rpm) × HTF (mm/min)	9	0.42533	0.047259	0.50	2.250131477	0.861	6.31 %
TRS (rpm) × LT (μm)	9	0.05996	0.006662	0.07	2.250131477	1.000	0.89 %
(mm/min) × LT (μm)	9	1.42998	0.158887	1.68	2.250131477	0.142	21.22 %
Error	27	2.5481	0.094374				37.82 %
Total	63	6.73731					100.00 %

4.1 Influence of input parameters on MRR

It was observed that when the HTF was increased from 40 to 100 mm/min, there is drastic and linear improvement in MRR as shown in Fig. 2. As the tool moves from left to right above the machining surface, only a small area of the tool tip will be near enough to the machining surface to produce spark. As the HTF is increased, the rate of unproductive movement of the tool will get reduced which, in turn, increases the MRR. Also from the ANOVA table, it can be observed that the contribution of horizontal feed rate of the tool is more significant in affecting MRR (Table 4).

Also, it can be observed from the ANOVA table that TRS and LT are also significant parameters of MRR. Increase in TRS resulted in drastic improvement of MRR till 750 rpm; further increase of rpm to 1500 rpm yielded appreciable progress in MRR, and when the speed was increased from 1500 to 2500, there was meager increment in MRR as seen in Fig. 2. The overall increase in MRR was caused by the effective debris removal from the inter-electrode gap due to the centrifugal force developed because of tool rotation. As the TRS was increased, the centrifugal force pushed the debris particles at higher speed out of the machining zone. As the speed increased to a higher level, the debris particles will hit the side walls of the channel, bounce back and forth between the tool and workpiece, and get trapped in between. Due to this reason, there is a small drop in the slope of MRR curve when TRS was increased above 1500 rpm.

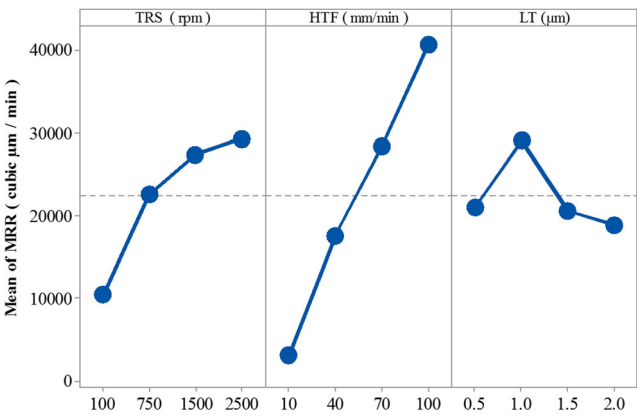

Fig. 2 Main effect plot of MRR

Maximum MRR was achieved when the LT was 1 μm as shown in Fig. 2. When the LT was very small, the distance between the tool and electrode gets smaller which affects the effective removal of debris; this may be the reason for very small MRR. When the LT was increased beyond 1 μm, the time taken for tool retraction would increase and also, the optimal gap condition for effective ionization of dielectric will be affected, and thus, MRR was reduced at higher values of LT. Also from the ANOVA table and Fig. 3, it can be observed that interaction of TRF versus HTF and also HTF versus LT is significant. There is no interaction between TRS versus LT because when the LT is increased, and there will be no effect of centrifugal force inside the micro-channel machining zone because the tool tip will be retracted far from the machining zone.

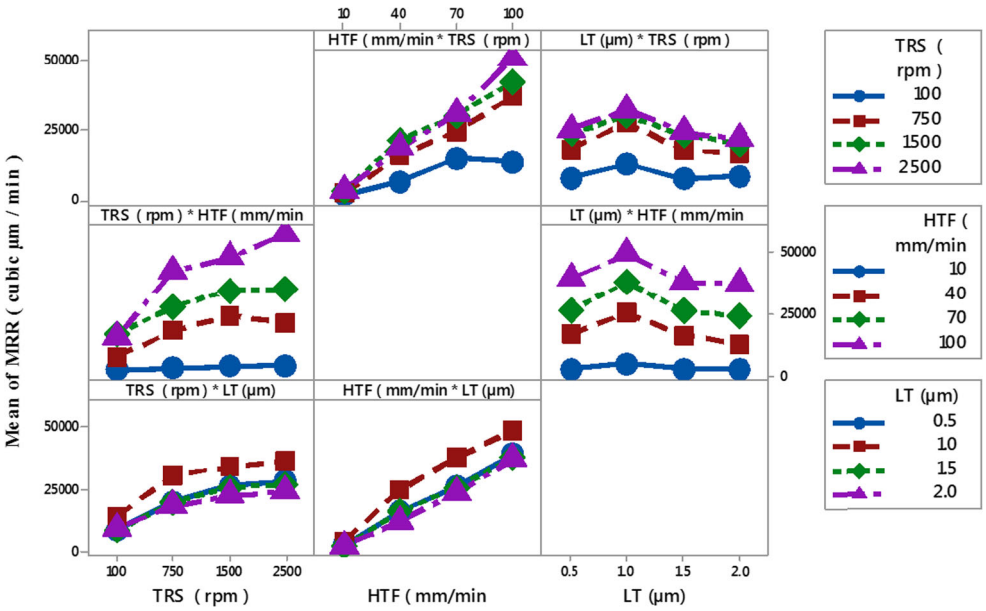

Fig. 3 Interaction plot of MRR

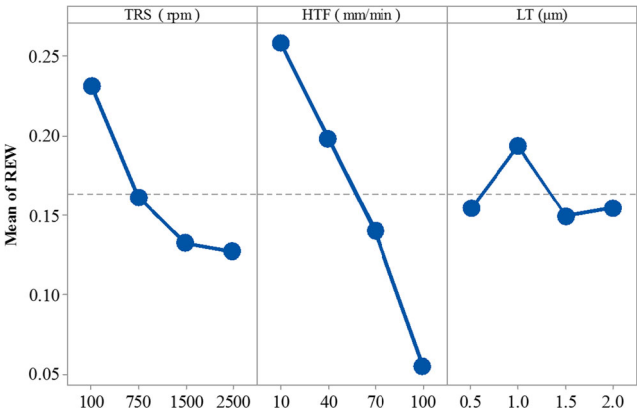

Fig. 4 Main effect plot of REW

4.2 Influence of input parameters on REW

As the TRF is increased from 100 to 2500 rpm, there is significant improvement in the ratio of REW (Figs. 4 and 5). Since there is very high MRR and low TWR in 2500 rpm, the value of REW is very small when compared to all other speeds. The value of REW also decreases gradually when HTF is increased from 10 to 70 mm/min. There is drastic decrease in the value of REW in 100 mm/min. The reason for such a huge improvement in tool life is that when HTF is increased, the tool tip was cleaned effectively from debris and carbon depositions due to the accompanied linear and

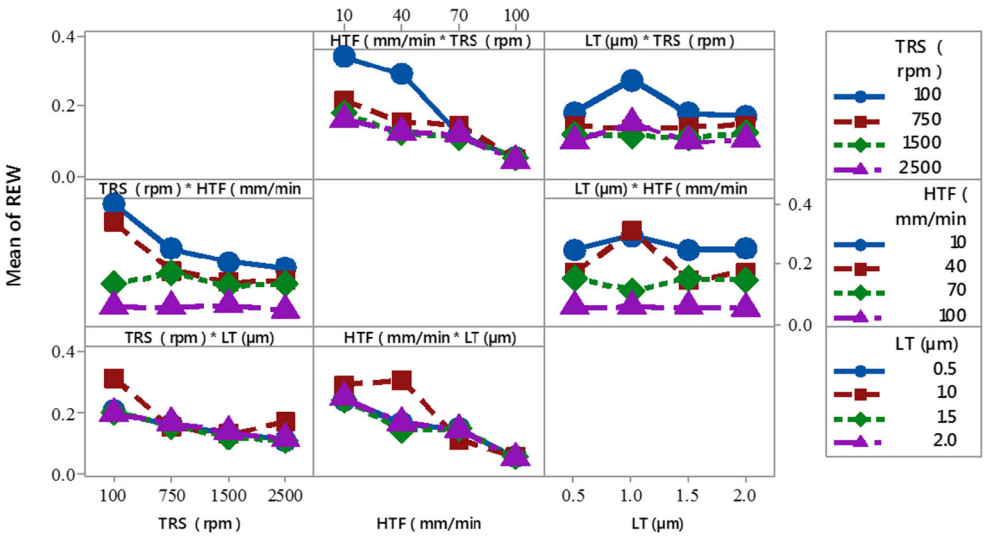

Fig. 5 Interaction plot of REW

centrifugal forces which lead in stable machining by avoiding unwanted short circuits.

The contour plots (Fig. 6a–f) and 3D surface plots (Fig. 7a–f) give more details on the behavior of MRR and REW with respect to different input parameters. The contour plot (Fig. 6a) shows the different regions of MRR with respect to the change in TRS versus HTF. The behavior of REW (Fig. 6b) is unique; it is influenced only by HTF. The contour plot (Fig. 6c, d) shows the influence of HTF versus LT on MRR and TWR; it clearly shows that the localized region of maximum MRR at LT of 1 μm, and REW remains the same at higher HTF for all

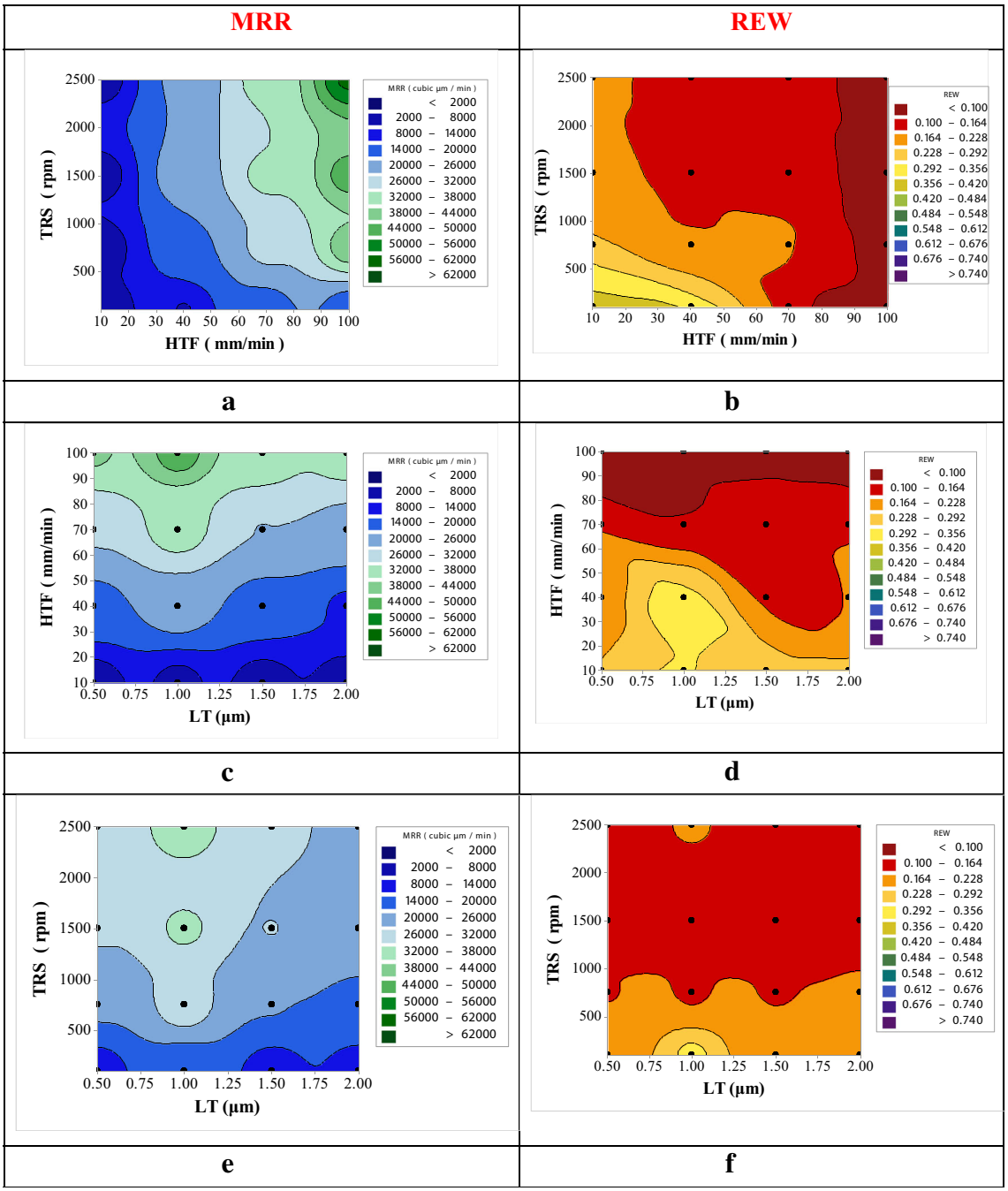

Fig. 6 Contour plots of MRR and REW

layer thickness values. Figure 6e shows a transition in MRR from low to high at LT of 1 μm, and it gets better when TRS is increased. It is recommended to use TRF >1000 rpm to get low REW (Fig. 6f).

In lower TRS, the MRR tends to increase linearly with respect to HTF and there is a meager drop at higher HTF (Fig. 7a) which is due to the effective amount of centrifugal force developed between the inter-electrode gap that removes the debris particles quickly. At lower TRS, the REW is also higher due to ineffective removal of debris particles (Fig. 7b). At layer thickness 1, there is higher MRR and REW (Fig. 7c–d) which follows the same pattern of the main effect plots (Figs. 3 and 4). The effect of HTF is higher in MRR than TRS (Fig. 7c, e). The contribution made by the interaction of LT versus HTF (Fig. 7d) is higher compared to LT versus TRS (Fig. 7f) which supports the ANOVA results.

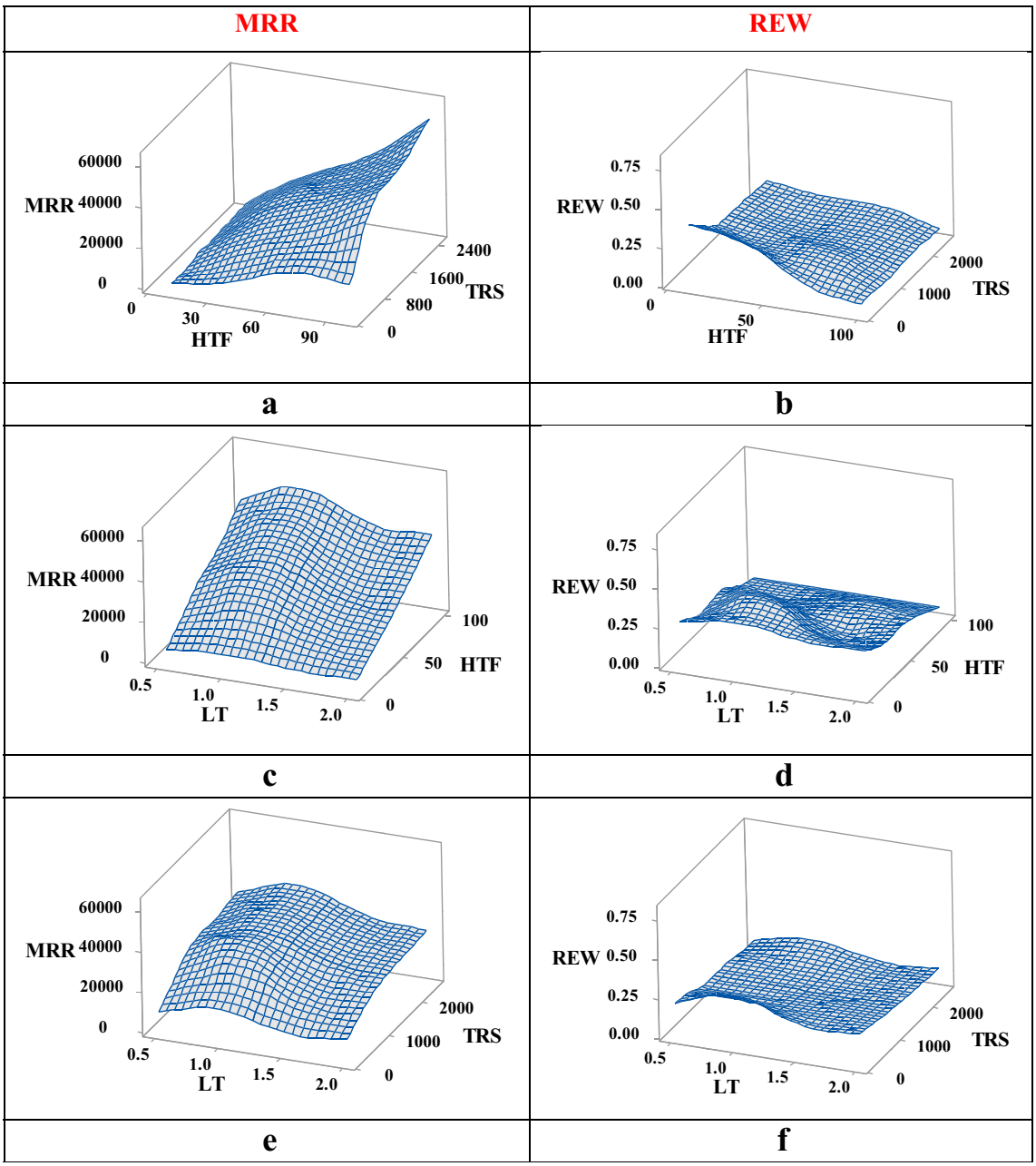

Fig. 7 3D surface plots of MRR and REW

4.3 Optimization of MRR and REW

Multiple responses can be optimized effectively by using desirability function ($D_i y_i$) which translates the scale of individual response to desirability scale which ranges from 0 to 1 (higher desirability) [23]. Based on the requirement, one can select any of the following desirability functions: (1) lower the better and (2) higher the better. In this study, lower the better was assigned to REW and higher the better was assigned for MRR.

$$D_i^{max} \quad y_i = \begin{cases} 0 & \\ \left(\frac{y_i - M}{N - M}\right)^a & if\ y_i < M \\ & if\ M \le y_i \le N \\ 1 & if\ y_i > N \end{cases} \tag{1}$$

$$D_i^{min} \quad y_i = \begin{cases} 0 & \\ \left(\frac{y_i - N}{M - N}\right)^a & if\ y_i > N \\ & if\ M \le y_i \le N \\ 1 & if\ y_i < M \end{cases} \tag{2}$$

where M is the upper bound value and N is the lower bound value.

'a' varies in between 0.1 to 10 subject to the shape of D_i.

The multi-objective optimization plot in Fig. 8 shows the optimal settings of LT (1 μm), TRS (2500 rpm) and HTF (100 mm/min) for lower REW and higher MRR.

5 Conclusions and future work

- Thus, from the experimental study, it is evident that the non-electrical parameters HTF, TRS, and LT influence the machining performance of μED milling.
- Higher TRS and maximum HTF are recommended for better MRR with minimum TWR.
- LT significantly influences MRR and TWR, and also, layer-by-layer machining approach dresses the tool automatically, and hence, it is recommended to consider it as an input parameter in μED milling.
- The impact of LT, HTF, and TRS on surface quality can be studied in the future.

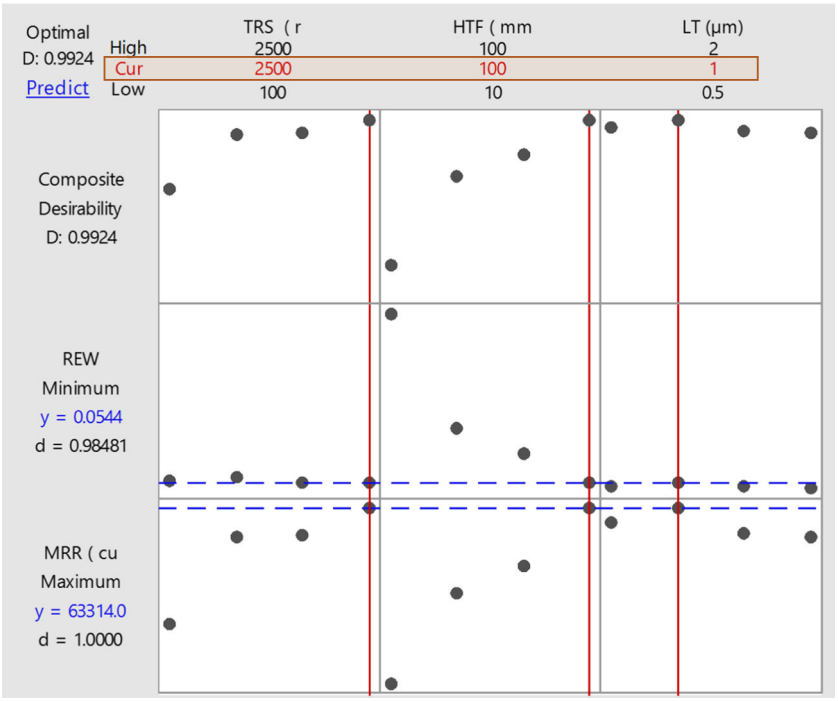

Fig. 8 Multi-objective optimization plot

References

1. Minh DN, Rahman M, Yoke SW (2013) Transitions of micro-EDM/SEDCM/micro-ECM milling in low-resistivity deionized water. Int J Mach Tools Manuf 69:48–56. doi:10.1016/j.ijmachtools.2013.03.008
2. Nguyen MD, Rahman M, Wong YS (2012) Enhanced surface integrity and dimensional accuracy by simultaneous micro-ED/EC milling. CIRP AnnManuf Technol 61:191–194. doi:10.1016/j.cirp.2012.03.011
3. Bissacco G, Tristo G, Hansen HN, Valentincic J (2013) Reliability of electrode wear compensation based on material removal per discharge in micro EDM milling. CIRP Ann Manuf Tech 62:179–182. doi:10.1016/j.cirp.2013.03.033
4. Karthikeyan G, Ramkumar J, Dhamodaran S, Aravindan S (2010) Micro electric discharge milling process performance: an experimental investigation. Int J Mach Tools Manuf 50:718–727. doi:10.1016/j.ijmachtools.2010.04.007
5. Jung JW, Jeong YH, Min BK, Lee SJ (2008) Model-based pulse frequency control for micro-EDM milling using real-time discharge pulse monitoring. J Manuf Sci Eng 130:4–6. doi:10.1115/1.2917305
6. Karthikeyan G, Garg AK, Ramkumar J, Dhamodaran S (2012) A microscopic investigation of machining behaviour in ED-milling process. J of Manuf Process 14:297–306. doi:10.1016/j.jmapro.2012.01.003
7. Song KY, Chung DK, Park MS (2010) Micro electrical discharge milling of WC-Co using a deionized water spray and a bipolar pulse. J Micromech Microeng 20:22–31. doi:10.1088/0960-1317/20/4/045022
8. Lin M, Tsao C, Hsu C, Chiou A, Huang P, Lin Y (2013) Optimization of micro milling electrical discharge machining of Inconel 718 by Grey-Taguchi method. Trans Nonferrous Mater 23:661–666. doi:10.1016/S1003-6326(13)62513-3
9. Wenwu Z (2010) Intelligent energy field manufacturing: interdisciplinary process innovations. CRC Press, USA
10. Vahid RA (2012) Net emission coefficient of plasma excited in the electrical discharge machining through liquid nitrogen dielectric medium. IEEE Trans Plasma Sci 40:853–862. doi:10.1109/TPS.2011.2182061
11. Banker KS, Oza AD, Dave RB (2013) Performance capabilities of EDM machining using aluminium, brass and copper for AISI 304L material. Int J Appl Innov Eng Manag 2:186–191
12. Banker KS, Parmar SP, Parekh BC (2013) Review to performance improvement of die sinking EDM using powder mixed dielectric fluid. Int J Res Mod Eng Emerg Tech 1:57–62
13. Moarrefzadeh A (2012) Study of workpiece thermal profile in electrical discharge machining (EDM) process. WSEAS Trans Appl Theor Mech 7:83–92
14. Kazimierz A, Karol M, Adam M, Stefan L, Marek M (1996) The temperature of a plasma used in electrical discharge machining. Plasma Sources Sci Tech 5:36–742. doi:10.1088/0963-0252/5/4/015
15. Zhao W, Gu L, Xu H, Li L, Xiang X (2013) A novel high efficiency electrical erosion process-blasting erosion arc machining. Procedia Eng 6:622–626. doi:10.1016/j.procir.2013.03.057
16. Liu Y, Wang J, Zhao, F, Wang, Y (2010) Research on dielectric breakdown mechanism of micro-EDM. Int Conference on Advanced Tech of Design and Manuf, 282–288. doi. 10.1049/cp.2010.1307
17. Richardson MT (2009) High resolution lithography—compatible micro-electro-discharge machining of bulk metal foils for micro-electro-mechanical systems. University of Michigan, Dissertation
18. Chang YF (2002) VSS controller design for gap control of EDM. JSME Int J Ser C, Mech Syst, Mach Elem Manuf 45:12–721. doi:10.1299/jsmec.45.712
19. Wong YS, Rahman M, Lim HS, Han H, Ravi N (2003) Investigation of micro-EDM material removal characteristics using single RC-pulse discharges. J Mater Process Tech 40:303–307. doi:10.1016/S0924-0136(03)00771-4
20. Rashed CA, Romoli L, Tantussi F, Fuso F, Bertoncini L, Fiaschi M (2014) Experimental optimization of micro-electrical discharge drilling process from the perspective of inner surface enhancement measured by shear-force microscopy. CIRP J Manuf Sci Tech 7:11–19. doi:10.1016/j.cirpj.2013.10.002
21. Dhanik S, Suhas SJ (2005) Modeling of a single resistance capacitance pulse discharge in micro-electro discharge machining. J Manuf Sci Eng 127:759–762. doi:10.1115/1.2034512
22. Dang M, Wong YS (2013) Transitions of micro-EDM/SEDCM/micro-ECM milling in low-resistivity deionized water. Int J Mach Tools Manuf 69:48–56. doi:10.1016/j.ijmachtools.2013.03.008
23. Mandal A, Dixit AR, Das AK, Mandal N (2015) Modeling and optimization of machining Nimonic C-263 Super Alloy using multi-cut strategy in WEDM. Mater Manuf Process. doi:10.1080/10426914.2015.1048462